Tensile Creep Behavior of Concrete Subject to Constant Restraint at Very Early Ages

Ya Wei[1] and Will Hansen[2]

Abstract: Tensile stress develops in concrete when shrinkage deformations and restraints (internal or external) exist. Utilization of appropriate creep or relaxation functions is crucial for assessing stress and the associated cracking potential in concrete, especially at early ages when chemical and physical properties change rapidly. The existing models, developed either from compressive creep tests or conventional tensile creep tests with constant loads applied at certain ages, were found to be unsuitable for such stress evaluation. This study was performed to investigate the restrained strain-stress development and tensile creep behavior of concrete subject to constant restraint starting at very early ages, which well represents field conditions of actual structures. Restrained stresses were measured using a specially designed frame. The concretes were cured and tested at two different temperatures (23°C versus 33°C) and ground granulated blast furnace slag contents (0% versus 30% of the total cementitious materials by mass). A modified tensile creep model is proposed to account for the high viscosity of concrete under constantly restrained conditions, allowing more accurate assessments of stress and cracking potential in structures such as slabs or pavements on the ground. **DOI: 10.1061/(ASCE)MT.1943-5533.0000671.**

CE Database subject headings: Concrete; Aging (material); Cracking; Stress; Creep.

Author keywords: Constant restraint; Early-age cracking; Restrained stress; Tensile creep; Viscous flow.

Introduction

Early-age cracking in concrete is generally a result of internal tensile stresses induced by restrained shrinkage other than external loading. Thermal dilation and autogenous shrinkage are considered the two major deformations leading to early-age cracking of concrete, affecting the durability of newly constructed or repaired structures. Stress assessment and cracking potential evaluation have attracted considerable interest in the concrete community [American Concrete Institute (ACI) 2010]. One of the most crucial factors in accurate shrinkage stress evaluation is the tensile creep or relaxation behavior of concrete, which is of significance especially for concrete loaded at early ages when massive relaxation might occur and varies with ages (Westman 1995; Altoubat and Lange 2001; Pane and Hansen 2008).

However, measuring tensile creep is a complicated task, especially on young concrete due to the simultaneous physical and chemical property variations at early ages (Altoubat and Lange 2001). The majority of past efforts focused on evaluating compressive creep testing data on hardened concretes (ACI 1992; Comité Euro-International du Béton-Fédération International de la Précontrainte (CEB-FIP) 1993; Bažant and Baweja 2000). However, the viscoelastic behavior of concrete under tension might be different from that under compression. The strong age-dependent properties of tensile creep have been found in concrete loaded within the first 24 h after setting. Modifications to existing compressive creep models have been made to satisfactorily capture the early-age tensile creep behavior (østergaard et al. 2001). In addition, microcracks might occur in such structures when the tensile stress/strength ratio exceeds the proportional limit, and this further complicates the linearity and the magnitude of creep deformations (Hossain and Weiss 2004).

Assessing the stress and cracking potential in concrete requires an appropriate tensile creep model capable of representing filed conditions. Tensile creep was conventionally measured on concrete under a constant load applied vertically at certain ages (østergaard et al. 2001; Pane and Hansen 2008). In some structures, such as newly constructed slabs on ground (Fig. 1), tensile stress might generate due to axial restraint right after set and grows slowly and continuously for a very long period of time. Stress evaluation of such structures requires a creep or relaxation function determined in a system subject to similar restraint conditions. For this purpose, this study was performed to measure the strain-stress development in axially restrained concrete specimens starting at very early ages using a specially designed frame. A creep compliance function is then indirectly determined based on the measured strain-stress data to account for the high-viscosity property. A relaxation model is proposed based on creep compliance analysis, allowing more accurate stress prediction and associated cracking potential evaluation in field structures. To investigate temperature and pozzolanic effects, concretes containing ground granulated blast furnace slag (GGBFS) were cured and tested at 23 and 33°C.

Determining Tensile Creep from Strain-Stress Measurements

Methodology

Before determining tensile creep compliance, both free strain and restrained stress should be known through measurement first.

[1]Lecturer, Key Laboratory of Civil Engineering Safety and Durability of China Education Ministry, Dept. of Civil Engineering, Tsinghua Univ., Beijing, 100084, China (corresponding author). E-mail: yawei@tsinghua.edu.cn

[2]Professor, Dept. of Civil and Environmental Engineering, 2340 G. G. Brown, Univ.of Michigan, Ann Arbor, MI 48109.

Note. This manuscript was submitted on February 1, 2012; approved on August 28, 2012; published online on August 31, 2012. Discussion period open until February 1, 2014; separate discussions must be submitted for individual papers. This paper is part of the ***Journal of Materials in Civil Engineering***, Vol. 25, No. 9, September 1, 2013. © ASCE, ISSN 0899-1561/2013/9-1277-1284/$25.00.

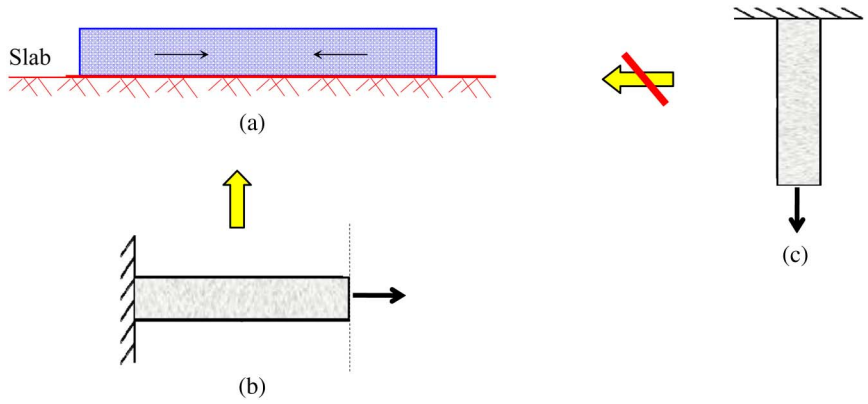

Fig. 1. Test method simulating field slab conditions: (a) side view of slab on ground; (b) top view of restrained shrinkage test where creep occurs; (c) side view of conventional tensile creep test under constant load

Tensile creep compliance is then indirectly calculated based on measured strain-stress development data. The procedure is detailed as follows.

The development of total shrinkage strain in a concrete after setting is written as

$$\varepsilon(t) = \varepsilon_{sh}(t) + \varepsilon_T(t) + \varepsilon_\sigma(t) = \varepsilon_{au}(t) + \alpha\Delta T(t) + \int_0^t J(t,t')d\sigma(t') \quad (1)$$

where $\varepsilon_{sh}(t)$ = shrinkage strain [it is autogenous shrinkage $\varepsilon_{au}(t)$ in this study for a sealed-cured condition]; $\varepsilon_T(t)$ = thermal strain; α = coefficient of thermal expansion of concrete; $\Delta T(t)$ = temperature change relative to zero-stress temperature; $\varepsilon_\sigma(t) = \int_0^t J(t,t')d\sigma(t')$ = strain due to stress increment applied at time t'; $J(t,t')$ = tensile creep compliance function.

For a fully restrained condition, however, the total shrinkage strain at time t should be zero. Thus, Eq. (1) becomes

$$\int_0^t J(t,t')d\sigma(t') = -[\varepsilon_{au}(t) + \varepsilon_T(t)] \quad (2)$$

in which $\int_0^t J(t,t')d\sigma(t')$ can be calculated numerically based on measured tensile stress increment $\Delta\sigma(t')$ applied at time t' and appropriate creep compliance function $J(t,t')$. $J(t,t')$ can represent existing models or a modification to existing models. The strain caused by stress at t_{i+1} is the summation of strain increments due to stress increment $\Delta\sigma_j$ applied during all the previous time intervals:

$$\int_0^t J(t,t')d\sigma(t') = \sum_{j=1}^{i} \Delta\varepsilon_j(t_{i+1}) = -\sum_{j=1}^{i} \Delta\sigma_j[J(t_{i+1},t_{j-1}) + J(t_{i+1},t_{j+1})] \quad (3)$$

By combining Eqs. (2) and (3), the tensile creep compliance $J(t,t')$ can be determined if $\Delta\sigma_j$, $\varepsilon_{au}(t)$, and $\varepsilon_T(t)$ are known. $\varepsilon_{au}(t)$ and $\varepsilon_T(t)$ can be obtained by either experimental measurements or predictions; $\Delta\sigma_j$ can be measured from restrained stress tests. Thus, the compliance function obtained represents the tensile creep behavior of concrete subject to sustained tension loading starting at very early ages. Moreover, two existing models as described subsequently will be used in Eq. (3) to verify whether they are appropriate for restrained stress assessment.

Existing Models

The B3 model is the mathematical expression of solidification theory-based structural creep law (Bažant and Baweja 2000). The theory found that the aging aspect was due to the growth of the volume fraction of the load-bearing portion of solidified matter whose properties are age independent (Bažant 1988; Bažant and Prasannan 1989). The B3 model was found to agree better with the experimental data. Its compliance function has the following form:

$$J(t,t') = \underbrace{q_1}_{\substack{instantaneous\\compliance}} + \underbrace{q_2 Q(t,t')}_{\substack{aging\ viscoelastic\\compliance}} + \underbrace{q_3\ \ln[1+(t-t')^n]}_{\substack{nonaging\ viscoelastic\\compliance}} + \underbrace{q_4\ \ln\left(\frac{t}{t'}\right)}_{\substack{flow\\compliance}} \quad (4)$$

The individual terms q_1, q_2, q_3, and q_4 in Eq. (4) are the empirical material constitutive parameters based on concrete strength and composition, which represent physically distinct components of creep, as indicated earlier, where $q_1 = 0.6 \times 10^6/E_{28}$; $q_2 = 185.4c^{0.5}f_c^{-0.9}$; $q_3 = 0.29(w/c)^4 q_2$; $q_4 = 20.3(a/c)^{-0.7}$; $n = 0.1$; $Q(t,t')$ is a function of t' and t; E_{28} = elastic modulus of concrete at 28 days; f_c = compressive strength at 28 days; c = cement content; w/c = water-to-cement ratio; and a/c = aggregate-to-cement ratio. Note that these parameters were calibrated with English units (inch-pounds).

The B3 model was developed from compressive creep test data on hardened concrete, and thus its application might be limited. A study by østergaard et al. (2001) showed that concrete exhibits high tensile creep strain if loaded at ages less than or equal to 1 day, and a modification to q_2 in B3 model to seize the very early-age high-viscoelastic behavior was proposed:

$$q_2' = q_2\left[\frac{t'}{t'-q_6}\right] \quad (5)$$

where q_6 = a new parameter introduced to capture the very high early-age creep, and it was considered as a structural setting time from liquid viscoelastic to solid viscoelastic status. The magnitude

J. Mater. Civ. Eng. 2013.25:1277-1284.

of q_6 will always be less than the earliest physical testing time. The østergaard model was found satisfactory in describing tensile creep behavior in concrete subject to a constant load applied at early ages. According to østergaard et al. (2001), the best fit value of q_6 equals 0.58 days for a loading age of 0.67 days, and the effect of the proposed correction vanishes after less than 3 days.

In this study, both the B3 model and østergaard's model are used to validate whether they are applicable for stress assessment in concrete subject to constant restraint. A more appropriate creep model will then be proposed based on these two models.

Experimental Strain-Stress Measurements and Analysis

Materials and Mixture Proportions

Type I ordinary portland cement (OPC) was used. As a supplementary cementitious material, GGBFS was used for evaluating the pozzolanic effect on early-age stress development and tensile creep behavior. The GGBFS was Grade 120, and the replacement level was 0% versus 30% of the total cementitious materials by mass. The chemical compositions of both the OPC and GGBFS are shown in Table 1.

This paper investigates concrete mixtures for particular applications such as concrete pavements or slabs on the ground. Therefore, typical pavement concrete mixture with a water/binder (w/b) ratio of 0.45 is used, and a target air content of $6.5 \pm 1.5\%$ is also adopted for pavement applications. The coarse aggregate used in the concrete mixture was crushed limestone with a maximum aggregate size of 12.5 mm. The fine aggregate was natural sand with a fineness modulus of 2.56. Since temperature was thought to affect creep properties at early ages (Hauggaard et al. 1999), concretes were cured and tested at two different temperatures of 23 and 33°C, respectively. For the case of 33°C, each material components were preconditioned prior to mixing by storing in an oven with temperature controlled at 33 ± 1°C. The mixture proportions and fresh properties of the concrete investigated are presented in Table 2.

Unrestrained and Restrained Shrinkage Test

Unrestrained and restrained shrinkage tests were conducted for assessing strain and stress development. In unrestrained tests, one-dimensional linear autogenous shrinkage was measured on sealed specimens using a double-walled, water-cooled, stainless-steel apparatus. The detailed testing procedure can be found elsewhere (Wei et al. 2011).

Table 1. Chemical Compositions of Cementitious Materials

Materials	OPC	GGBFS
Blaine fineness (cm^2/g)	4290	6020
SiO_2 (%)	20.4	37.49
Al_2O_3 (%)	5.04	7.77
Fe_2O_3 (%)	2.51	0.43
CaO (%)	62.39	37.99
MgO (%)	3.43	10.69
SO_3 (%)	2.75	3.21
Na_2O (%)	0.25	0.28
K_2O (%)	0.67	0.46
Total as oxides	97.47	—
C_3S	53.66	—
C_2S	18.01	—
C_3A	9.11	—
C_4AF	7.64	—

Notes: OPC = ordinary Portland cement; GGBFS = ground granulated blast-furnace slag.

Table 2. Proportions of Concrete Mixtures (kg/m^3)

Mixture name	O-1	O-2	G-1	G-2
Cement	451	451	316	316
GGBFS	0	0	135	135
Water	203	203	203	203
Limestone	402	402	402	402
Sand	1143	1143	1143	1143
AEA	1.5	1.5	1.2	1.2
Fresh air content (%)	8	6.5	7.4	6
Slump (mm)	70	65	79	58
Fresh temperature (°C)	24.2	32.6	22	32.2
Curing and testing temperature (°C)	23	33	23	33

Note: GGBFS = ground granulated blast furnace slag; AEA = air-entraining admixture.

The restrained shrinkage test measures stress development in an axially restrained concrete using a horizontal testing frame or temperature stress testing machine (TSTM) built for this purpose (Fig. 2). The TSTM was initially used to measure autogenous shrinkage and the induced stresses (Paillere et al. 1989) and was later employed to study the tensile viscoelastic behavior of concrete (Kovler et al. 1999; Choi and Oh 2010).

The frame used in this study is composed of a load cell and an actuator with servohydraulic control. One grip is fixed to the load cell and the other one is connected to the actuator for free movement. To provide a sufficient restraint condition and to avoid drift over a long period of time, the actuator was computer controlled to move cyclically relative to its original position. The cycles for the length adjustments are such that the amplitude of movement is relatively small (smaller than 1 to 5 μm for a 1,000-mm-long specimen), so that the concrete can be assumed to be under a "full-restraint" condition (Bentur and Kovler 2003). This type of frame is known as an active restraining rig for achieving a full restraint, which is independent of the restraining rigidity of the testing rig (Springenschmid et al. 1994; Bentur and Kovler 2003). In this study, the actuator was controlled to move cyclically at an amplitude smaller than 3 μm relative to its original position and at a time interval of 2 s. The specimen was directly cast into the foam-insulated mold already positioned in the test rig. Two ends of the specimen were enlarged to ensure a uniform stress distribution at the central part. A thin vinyl sheet was placed between the specimen and the mold to avoid frictional resistance. Immediately after casting, the upper surface of the specimen was covered with a plastic sheet to prevent any water evaporation. The mold was equipped with copper pipes that could circulate constant-temperature (23 ± 1°C or 33 ± 1°C) water from a heating-cooling control bath. During the entire testing period, the specimen was sealed cured. The temperature field in the specimen was measured at three locations along the specimen depth. It was found that the specimens had a quite uniform temperature distribution along the depth at all times. The stress measurements started immediately after casting.

Analysis of Stress Development in Restrained Concrete

In concrete, both thermal- and moisture-related deformations contribute to early-age stress development. For the sealed-cured specimens investigated in this study, the development of early-age stress was a result of restrained thermal and autogenous deformations.

J. Mater. Civ. Eng. 2013.25:1277-1284.

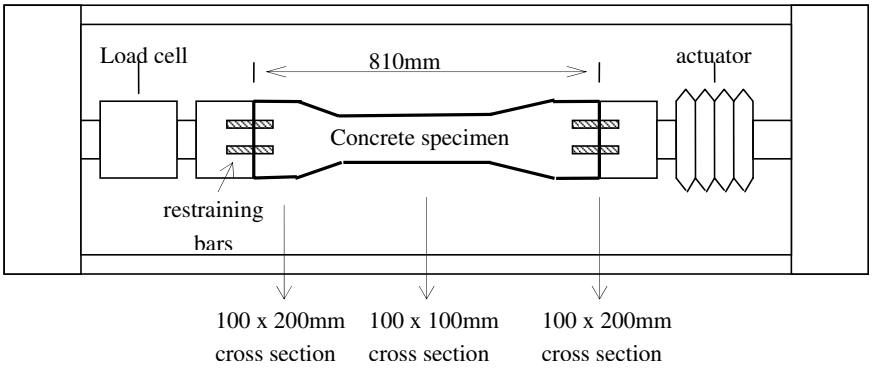

Fig. 2. Top view of restrained shrinkage test

The typical curves of temperature, strain, and stress developments are shown in Fig. 3 for the O-1 mixture. It was found that the restrained stress was induced a few hours after casting. A thermal effect dominated the compressive stress development. The temperature increased from the mixing temperature to the maximum due to cement hydration and was then stabilized at the end of the first day, indicating that autogenous shrinkage would be the major driving force thereafter for tensile stress development.

In Fig. 3(a), $T_{zero\text{-}stress}$ is the temperature where the corresponding restrained stress switches from compression to tension. After $T_{zero\text{-}stress}$, any temperature drop and shrinkage deformations, if restrained, will generate tensile stress. Correspondingly, $\varepsilon_{zero\text{-}stress}$, shown in Fig. 3(b), is defined in this study as the strain where the corresponding restrained stress switches from compression to tension. $\varepsilon_{zero\text{-}stress}$ was used as the starting point of shrinkage deformation for the purpose of tensile creep evaluation. It should be noted that $\varepsilon_{zero\text{-}stress}$ is not necessarily zero because, as a result of the high relaxation property of young concrete, most of the compressive stress being relaxed and a rapid stress transformed from compression to tension.

The measured free autogenous shrinkage and restrained stress developments are shown in Fig. 4 for the four mixtures investigated. It can be seen that none of the tests caused failure of the concrete specimens during the testing period. Stress developments closely followed strain developments. For concrete mixtures with $w/c = 0.45$, the autogenous shrinkage was expected to be small. It was approximately 50 μm for the OPC system and 100 μm for the GGBFS system at the age of 12 days. However, a high curing temperature (33°C) resulted in faster and greater strain and stress developments because cement hydration and self-desiccation were

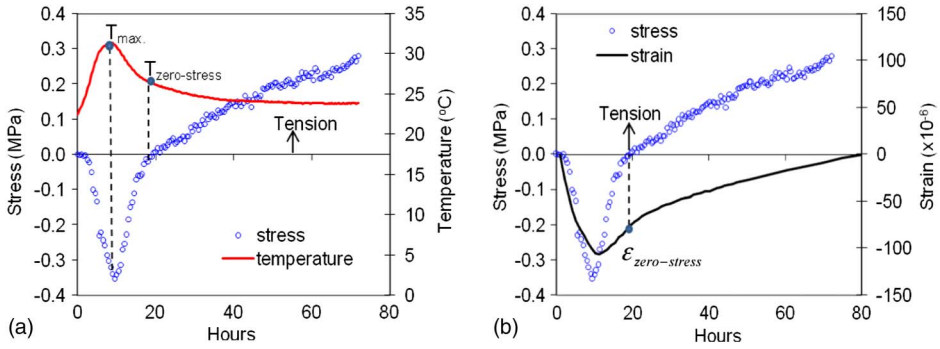

Fig. 3. Typical curves of (a) temperature and stress developments; (b) strain and stress developments in a sealed-cured concrete

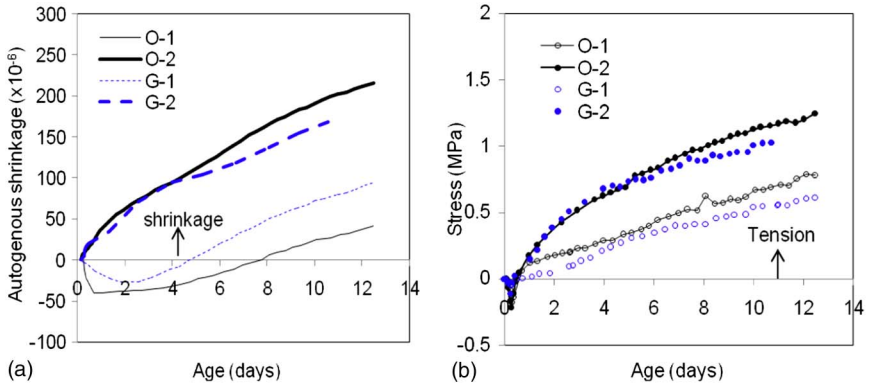

Fig. 4. Measured autogenous shrinkage and restrained stress of four concrete mixtures

J. Mater. Civ. Eng. 2013.25:1277-1284.

accelerated under the high temperature conditions. In the same curing temperature conditions, 30% of the GGBFS showed a minor effect on strain and stress development.

For tensile creep analysis, the shrinkage deformation relative to $\varepsilon_{\text{zero-stress}}$, the associated tensile stress, and the direct tensile strength of the four concrete mixtures are shown in Fig. 5. It can be seen that the induced tensile stress from restrained thermal and autogenous shrinkage deformations could be significant. The tensile stress/direct tensile strength ratio could exceed 60% at later ages. A ratio of the tensile stress to strength is generally used to indicate how close a concrete might fail even if cracking is not observed (Hossain and Weiss 2004). It was suggested that a stress ranging from 60 to 70% of the tensile strength is considered to be the limit for concrete to develop cracks or fail in the restrained condition (Shah et al. 1998; Igarashi et al. 2000; Kristiawan 2005). Therefore, sustained tensile stress might cause premature microcracking, which can induce a large amount of later-age creep in the concretes investigated in this study.

Direct tensile strength should be used in cracking potential evaluation because it is more representative than split tensile strength. Note that the direct tensile strength shown in Fig. 5 was determined by breaking the specimen at various ages using the TSTM (Fig. 2). The split tensile strength was measured on cylinder specimens with dimensions of Φ 100 × 200 mm. The relationship between direct tensile strength and split tensile strength is shown in Fig. 6. It can be seen that the ratio of these two is approximately 0.8. Sanjayan (2008) found that this ratio was in the range of 0.85–0.87. Altoubat and Lange (2001) found the ratio to be approximately 0.6–0.72 for OPC concrete with a w/c of 0.5.

From Fig. 5, the measured restrained stress is significantly reduced as compared to the elastic stress. Therefore, it is suspected that the continuous restraint to shrinkage deformations starting at very early ages could induce a large stress relaxation. Igarashi et al. (2000) also found large creep deformation in the restrained autogenous shrinkage test and concluded that this behavior was typical for loading at very early ages. The creep property of concrete depends on many factors, and the age of the concrete at the time of loading, the loading rate, and the w/c ratios are all important ones. Another important factor contributing to large creep might be the "flow" property of an axially restrained concrete. Like plastic flow, flow in a solid is found to be a consequence of stress differences at different locations (Reiner 1949). For a restrained specimen, as shown in Fig. 2, the local autogenous shrinkages reach equilibrium at all times due to the fact that autogenous shrinkage is a material-related property and independent of conditions such as structure geometry and external restraint. However, there exists a delay of local shrinkage stress equilibrium at different locations due to the external and internal restraints. This will cause a stress difference at different locations, and thus flow develops in such restrained concrete.

Modified Creep Model for Concrete Subject to Constant Restraint at Very Early Ages

Modified Compliance Function from Strain-Stress Measurement

As mentioned previously, the tensile creep behavior of concrete subject to constant restraint is suspected of being different from that measured by a conventional tensile creep test. Evaluations using the B3 model and østergaard's model were conducted to validate whether these two models are appropriate for describing the tensile creep behavior of concrete subject to constant restraint. According to Fig. 7, neither of the two models produces accurate shrinkage strain prediction for all mixtures. østergaard's model prediction fits well with the measured strain at early ages (less than approximately 3 days) because of the modification made to incorporate the high early-age creep [Eq. (5)]. For later-age strain prediction, both the B3 model and østergaard's model underestimate the creep strain of concrete subject to constant restraint. This might be due mainly to the fact that these two models

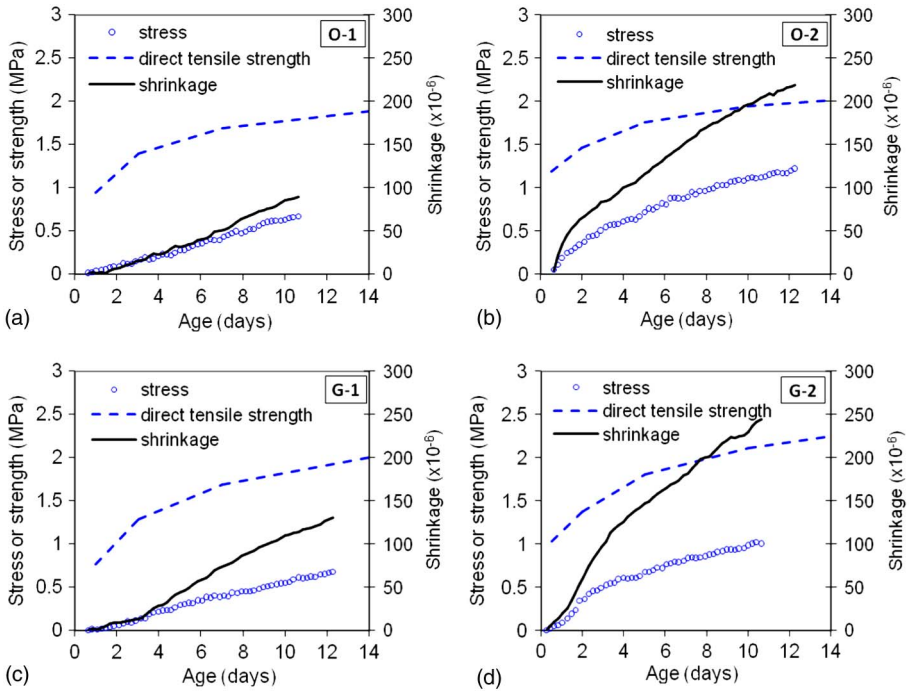

Fig. 5. Relationship between shrinkage, stress, and direct tensile strength developments of four concrete mixtures

J. Mater. Civ. Eng. 2013.25:1277-1284.

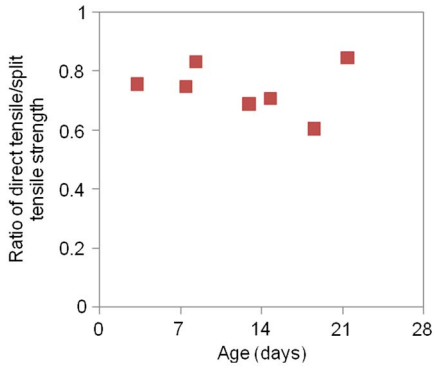

Fig. 6. Relationship between direct tensile and split tensile strength of concrete

were developed based on a conventional creep test without a sustained restraint condition and microcracking in the concrete involved.

Since østergaard's model captures early-age tensile creep behavior well, a further modification based on this model is preferable to account for both high early-age and later-age creep of concrete subject to constant restraint. According to Bažant et al. (1997), long-term creep is mostly a consequence of the relaxation of microprestress in the micropores of cementitious materials, leading to a viscous flow of concrete. For concrete subject to sustained tension, the relaxation of microprestress is expected to grow continuously as new hydrates are produced. At the macroscopic level, this movement within the micropores of concrete is accounted for by the flow creep strain. Therefore, the long-term large creep in an axially restrained specimen should be exhibited by the flow term in the creep model.

By observing Eq. (4), to account for the high later-age creep caused by the "flow" behavior of concrete, it is reasonable to modified the flow parameter q_4 by the parameter q_7, as shown in the following equation:

$$J(t,t') = q_1 + q_2\left[\frac{t'}{t'-q_6}\right]Q(t,t') + q_3\,\ln[1+(t-t')^n] + q_4 \cdot q_7\,\ln\left(\frac{t}{t'}\right) \quad (6)$$

q_7 is expected to be greater than 1 to account for the long-term flow creep. The predicted strain using the modified model [Eq. (6)] agrees well with the measured strain, as shown in Fig. 7. The values of q_6 and q_7 are calculated and listed in Table 3 for each mixture. From Table 3, $q_6 = 0$ for the O-1 and O-2 mixtures, and $q_6 = 0.5$ for the G-1 and G-2 mixtures. According to østergaard et al. (2001), q_6 is considered as a structural setting time from liquid to solid viscoelastic, and larger value of q_6 indicates a higher early-age creep. The results show that parameter q_6 is sensitive to cementitious material types, and concrete containing 30% GGBFS results in slightly greater early-age tensile creep. On the other hand, the curing temperature has a minor effect on parameter q_6 and, correspondingly, early-age tensile creep due to the relative short-time period that temperature can affect. From Table 3, $q_7 = 8$ for the O-1 and O-2 mixtures, and $q_7 = 15$ and 12 for the G-1 and G-2 mixtures, respectively. The greater the magnitude of q_7, the larger the flow creep of the concrete. The calculated results of q_7 indicate that q_7 is sensitive to cement type, and concrete containing GGBFS has greater later-age flow deformation as well. The temperature effect on q_7 is minor. In addition to the flow component, the parameter q_7 in the modified creep model might be able to take the microcracking effect into account when the measured stress/strength ratio approaches the proportional limit.

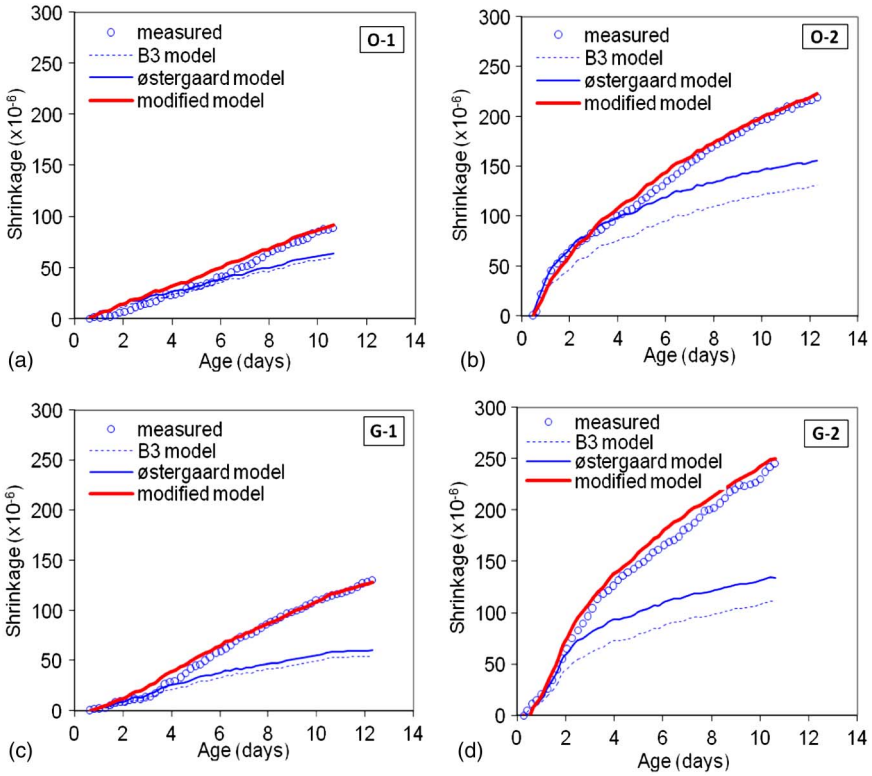

Fig. 7. Prediction of shrinkage deformation from measured stresses using different creep models

J. Mater. Civ. Eng. 2013.25:1277-1284.

Table 3. Parameters for Creep Compliance and Relaxation Modulus Prediction

Mixture	q_6	q_7	d_1	d_2	p
O-1	0	8	0.526	0.977	0.731
O-2	0	8	0.502	0.947	0.683
G-1	0.5	15	0.380	0.747	0.901
G-2	0.5	12	0.440	0.877	0.795

Note: q_6, q_7 are parameters as shown in Eq. (6); d_1, d_2, and p are parameters as shown in Eq. (11).

Relaxation Modulus Based on Modified Compliance Function

For stress evaluation, the relaxation modulus $R(t,t')$ must be known. This can be done by transforming the creep compliance $J(t,t')$ into a relaxation modulus by solving the volterra integral equation (Neville et al. 1983):

$$\int_0^t J(t,t')dR(t') = 1 \tag{7}$$

Solving Eq. (7) requires that $J(t,t')$ be a function with parameters either fixed or a continuous function of age. A log-power form function is found to be suitable for the modified creep compliance function because it was shown to be very simple yet accurate and at the same time produces a nonnegative relaxation modulus (Pane and Hansen 2008). It is expressed as

$$J(t,t') = \frac{1}{E(t')} + p_1 \ln[1 + p_2(t')(t-t')^{p_3}] \tag{8}$$

where $1/E(t')$ = instantaneous compliance; p_1 and p_3 = material constants to be determined; $p_2(t')$ varies with age and can be written as

$$p_2(t') = c_1 t'^{-c_2} \tag{9}$$

Eq. (7) was then numerically solved for $R(t')$ using a trapezoidal integration scheme:

$$R(t,t') = -\frac{\sum_{i=1}^{k-1}[J(t_k,t_i)+J(t_k,t_{i-1})-J(t_{k-1},t_i)-J(t_{k-1},t_{i-1})]\Delta R(t_i)}{J(t_k,t_k)+J(t_k,t_{k-1})} \tag{10}$$

The relaxation modulus calculated is shown in Fig. 8 as the dotted lines, which can be fitted using a hyperbolic relaxation function as the solid lines shown in Fig. 8:

$$R(t,t') = E(t')\left[1 - \frac{\left[\frac{t-t'}{d_1 t'^{d_2}}\right]^p}{1+\left[\frac{t-t'}{d_1 t'^{d_2}}\right]^p}\right] \tag{11}$$

where $E(t')$ = elastic modulus at time t'; the set of parameters d_1, d_2, and p, which give the best fit with the experimental data, are tabulated in Table 3.

After obtaining the relaxation modulus, the restrained tensile stress in concrete can be calculated numerically using the following equation:

$$\sigma(t_{i+1}) = \sum_{j=1}^{i}\Delta\sigma_j(t_{i+1}) = \sum_{j=1}^{i} -\frac{\alpha_t\Delta T_j + \Delta\varepsilon_j}{2}[R(t_{i+1},t_{j-1}) + R(t_{i+1},t_{j+1})] \tag{12}$$

The modified tensile creep and relaxation modulus functions allow for a more accurate assessment of the shrinkage stress and cracking potential in newly constructed structures or repairs.

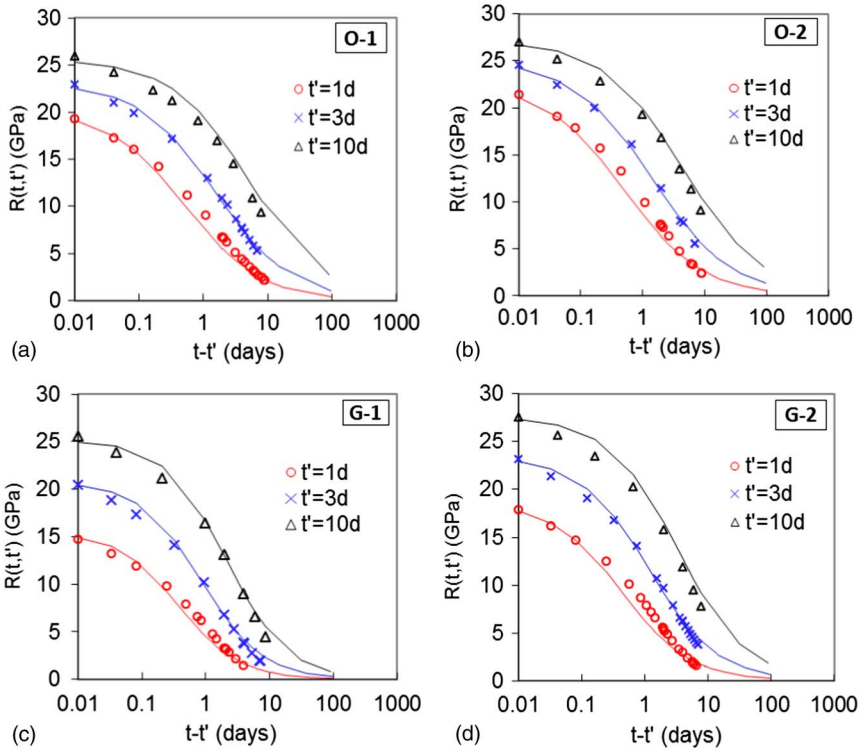

Fig. 8. Relaxation modulus calculated from modified creep model

J. Mater. Civ. Eng. 2013.25:1277-1284.

Conclusions

This study was performed to investigate the strain-stress developments and viscoelastic behaviors of concrete subject to constant restraint starting at very early ages. The constantly restrained specimens tested in this study well represent the field conditions of actual structures. The concretes were cured and tested at two different temperatures (23 and 33°C) and GGBFS contents (0 and 30% of the total cementitious materials by mass). The major findings are as follows:

1. The restraint to thermal and autogenous deformations caused high internal stress. The induced tensile stress/strength ratio could exceed 60%, where premature microcracking may occur. A high curing temperature caused faster and greater strain and stress developments. GGBFS did not significantly affect strain-stress development during the testing period of 12 days of this study.
2. Continuous restraint to concrete shrinkage deformation starting at very early ages induced a large tensile creep strain. The viscous behavior of concrete under a sustained tension load was different from that of a conventional tensile creep test. The creep behavior under such conditions was complicated by the very early-age and sustained load application, viscous flow, and potential microcracking in concrete. The restrained shrinkage stress could not be predicted accurately by the existing models, which are based on conventional tests with constant loads applied at certain ages.
3. A creep compliance function was determined indirectly from restrained strain-stress measurements. The new function was modified based on solidification theory, incorporating a high viscous flow property and possible microcracking effect of a constantly restrained concrete by the parameter q_7. From the modified compliance function, concrete containing GGBFS showed higher early-age and flow creep deformation. Such a blended system also showed sensitivity to temperature effects on flow creep under a sustained tension load.
4. The modified compliance and relaxation modulus functions allowed for more accurate assessment of shrinkage stress and cracking potential in newly constructed structures and repairs. However, it should be noted that this paper provided only a limited amount of experimental evidence, and the conclusions should be regarded as preliminary. More experiments on the effects of w/c ratios or other factors are needed for verification.

Acknowledgments

This material is based on work supported by the National Science Foundation of China under Grant 51108246. Any opinions, findings, and conclusions or recommendations expressed in this material are those of the author(s) and do not necessarily reflect the views of the National Science Foundation.

References

Altoubat, S. A., and Lange, D. A. (2001). "Tensile basic creep: Measurements and behavior at early age." *ACI Mater J.*, 98(5), 386–393.

American Concrete Institute (ACI). (1992). *Prediction of creep, shrinkage and temperature effect in concrete structures (ACI 209R-92)*, Detroit.

American Concrete Institute (ACI). (2010). *Report on early-age cracking: Causes, measurement, and mitigation (ACI 231R-10)*, Detroit.

Bažant, Z., Hauggard, A., Baweja, S., and Ulm, F.-J. (1997). "Microprestress solidification theory for concrete creep. I: Aging and drying effects." *J. Eng. Mech.*, 123(11), 1188–1194.

Bažant, Z. P. (1988). "Material models for structural creep analysis." *Proc., RILEM Conf. on Mathematical Modeling of Creep and Shrinkage of Concrete*, Wiley, New York.

Bažant, Z. P., and Baweja, S. (2000). *Creep and shrinkage prediction model for analysis and design of concrete structures: Model B3, ACI SP–194*, American Concrete Institute, Detroit, 1–83.

Bažant, Z. P., and Prasannan, S. (1989). "Solidification theory for concrete creep. II: Verification and application." *J. Eng. Mech.*, 115(8), 1691–1703.

Bentur, A., and Kovler, K. (2003). "Evaluation of early age cracking characteristics in cementitious systems." *Mater. Struct.*, 36(3), 183–190.

Choi, S. C., and Oh, B. H. (2010). "New viscoelastic model for early-age concrete based on measured strains and stresses." *ACI Mater. J.*, 107(3), 239–247.

Comité Euro-International du Béton-Fédération International de la Précontrainte (CEB-FIP). (1993). *Model Code 1990, CEB Bulletin 213/214*, Paris.

Hauggaard, A. B., Damkilde, L., and Hansen, P. F. (1999). "Transitional thermal creep of early age concrete." *J. Eng. Mech.*, 125(4), 458–465.

Hossain, A. B., and Weiss, J. (2004). "Assessing residual stress development and stress relaxation in restrained concrete ring specimens." *Cem. Concr. Compos.*, 26(5), 531–540.

Igarashi, S., Bentur, A., and Kovler, K. (2000). "Autogenous shrinkage and induced restraining stresses in high-strength concretes." *Cem. Concr. Res.*, 30(11), 1701–1707.

Kovler, K., Igarashi, S. I., and Bentur, A. (1999). "Tensile creep behavior of high strength concretes at early ages." *Mater. Struct.*, 32(219), 383–387.

Kristiawan, S. A. (2005). "Tensile stress-strain behavior of concrete under various rates of loading and the role of creep on the behavior." *J. Teknik Sipil*, 6(1), 73–81.

Neville, A. M., Dilger, W. H., and Brooks, J. J. (1983). *Creep of plain and structural concrete*, Construction Press, New York.

østergaard, L., Lange, D., Altoubat, S. A., and Stang, H. (2001). "Tensile basic creep of early-age concrete under constant load." *Cem. Concr. Res.* 31(12), 1895–1899.

Paillere, A. M., Buil, M., and Serrano, J. J. (1989). "Effect of fiber addition on the autogenous shrinkage of silica fume concrete." *ACI Mater. J.*, 86(2), 139–144.

Pane, I., and Hansen, W. (2008). "Predictions and verifications of early-age stress development in hydrating blended cement concrete." *Cem. Concr. Res.*, 38(11), 1315–1324.

Reiner, M. (1949). "On volume or isotropic flow as exemplified in the creep of concrete." *Appl. Sci. Res.*, 1(1), 475–488.

Sanjayan, T. (2008). "Factors contributing to early age shrinkage cracking of slag concretes subjected to 7-days moist curing." *Mater. Struct.*, 41(4), 633–642.

Shah, S. P., Ouyang, C., Marikunte, S., Yang, W., and Becq-Giraudon, E. (1998). "A method to predict shrinkage cracking of concrete." *ACI Mater. J.*, 95(4), 339–346.

Springenschmid, R., Breitenbucher, R., and Mangold, M. (1994). "Development of the cracking frame and the temperature-stress testing machine." *Thermal cracking in concrete at early ages, Proc. RILEM Symp.*, R. Springenschmid, ed., E & FN Spon, London, 137–144.

Wei, Y., Hansen, W., Biernacki, J. J., and Schlangen, E. (2011). "Unified shrinkage model for concrete from autogenous shrinkage test on paste with and without GGBFS." *ACI Mater. J.*, 108(1), 13–20.

Westman, G. (1995). "Basic creep and relaxation of young concrete." *Thermal cracking in concrete at early ages, Proc., Int. RILEM Symp.*, R. Springenschmidt, ed., E&FN Spon, London, 87–94.

J. Mater. Civ. Eng. 2013.25:1277-1284.